9302 *Macromolecules* **2004,** *37,* 9302−9304

# Probing Fickian and Non-Fickian Diffusion of $CO_2$ in Poly(methyl methacrylate) Using in Situ Raman Spectroscopy and Microfocus X-ray Computed Tomography

**Ji-Ho Yoon,**[*,†,⊥] **Taro Kawamura,**[†] **Satoshi Takeya,**[†]
**Shigeki Jin,**[†] **Yoshitaka Yamamoto,**[†]
**Takeshi Komai,**[†] **Masayoshi Takahashi,**[†]
**A. Victoria Nawaby,**[‡] **and Y. Paul Handa**[*,§]

*National Institute of Advanced Industrial Science and Technology, Tsukuba, Ibaraki 305-8569, Japan; Institute for Chemical Processes and Environmental Technology, National Research Council of Canada, Ottawa, Ontario, Canada K1A 0R6; and Technology Center, Pactiv Corporation, Canandaigua, New York 14424-7990*

*Received June 24, 2004*
*Revised Manuscript Received October 24, 2004*

Poly(methyl methacrylate) (PMMA) and poly(ethyl methacrylate) (PEMA) in contact with compressed $CO_2$ at suitable conditions are known to exhibit the unusual retrograde vitrification;[1−6] that is, they undergo rubber-to-glass transition on heating. This phenomenon arises due to the rather high solubility, over 30 wt %, of the gas at subambient temperatures coupled with a rapid decrease in the solubility on heating. An important feature of these systems is that ultramicrocellular or nanocellular foams can be readily obtained under mild temperature and pressure conditions.[7,8] These cellular materials have potential applications in electronics, thermal insulation, environmental remediation, membrane separation, and drug delivery systems. An understanding of the mechanism of molecular diffusion of $CO_2$ in polymers is key to development of processes for making specialty cellular materials.

The diffusion behavior of a penetrant in polymers has been studied extensively, both theoretically and experimentally. Diffusion of a penetrant in a rubbery polymer is often Fickian, whereas in a glassy polymer, diffusion can exhibit non-Fickian (or anomalous) behavior, especially when there is extensive swelling of the polymer matrix with the penetrant. Previous studies on the diffusion behavior of $CO_2$ in polymers were directed at measuring swelling and sorption/desorption kinetics by gravimetric techniques[6,8−12] and, in some cases, at directly observing the diffusion front using optical methods.[11−15] The PMMA−$CO_2$ system has been well characterized in terms of solubility and diffusivity using the gravimetric method.[6−8] In this Communication, we report the first use of in-situ Raman spectroscopy and microfocus X-ray computed tomography (X-ray CT) to probe and assess the diffusion behavior of $CO_2$ in PMMA.

A Raman spectrometer (Jobin Yvon Ramanor T64000) with a triple monochromator of 1800 grooves/mm grating and a CCD detector were used in this work. An Ar ion laser source emitting a 514.5 nm line was used with a power of 200 mW. The scattered radiation was collected at 180° geometry with a slit width of 250 μm. Spherical PMMA particles ($M_w$ = 116 000) with an average diameter of about 200 μm were obtained from Sumitomo Chemical Co. For the diffusion studies, the PMMA sample was placed into a thermostated high-pressure cell with a volume of approximately 2 $cm^3$ and equipped with a sapphire window. After evacuation, the cell was quickly pressurized to initiate diffusion of $CO_2$ into the polymer matrix. During the runs, the system pressure was kept constant using a pressure control unit and a metering valve. The cellular morphologies were produced by conditioning 6 mm spherical samples (also from Sumitomo Chemical Co.) at 273 K and 3.0 MPa with $CO_2$ for various times and then quickly transferring the samples into a water bath at 95 °C. Structural images of the foamed PMMA samples were investigated with a microfocus X-ray CT scanner (Shimadzu, SMX-225CTS). The entire 6 mm foamed sample was used for imaging. During measurements of the two-dimensional structural images, a cone-shaped X-ray beam was emitted from a 4 μm aperture while the samples placed on rotation goniometer rotated through 360° for 10 min radiation. The apparatus had a spatial resolution of approximately 30 μm because of the use of a high-resolution image intensifier detector.

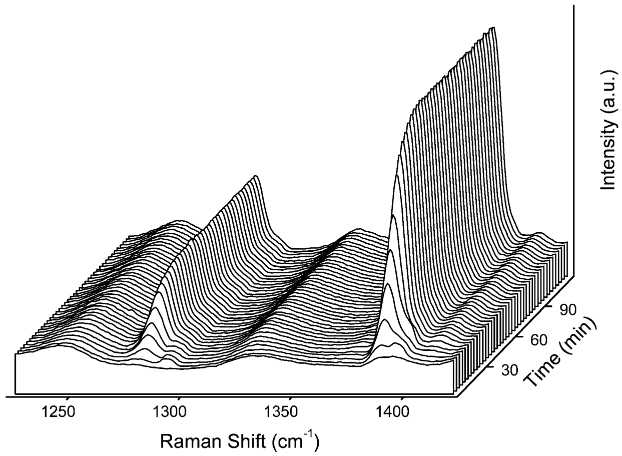

**Figure 1.** Time-resolved Raman spectra for $CO_2$ molecules in the gas phase and dissolved in PMMA at 273 K and 3 MPa.

Figure 1 shows the time-resolved Raman spectra for the PMMA−$CO_2$ system at 273 K and 3 MPa. An interesting feature of Raman spectroscopy is that signatures of the $CO_2$ molecules in different environments are easily observed. The characteristic Raman bands of $CO_2$ molecules in the gas phase are observed at 1287 and 1390 $cm^{-1}$. In addition, two dominant peaks located at 1279 and 1385 $cm^{-1}$ attributable to dissolved $CO_2$ molecules are also observed.[16] At short times, these peaks were relatively weak and, therefore, could not be clearly distinguished from those due to $CO_2$ in the gas phase. At longer elapsed times, a sharp increase in the intensity of the peaks for dissolved $CO_2$ was observed. After about 30 min, the relative intensity did not change much, indicating establishment of equilibrium between gaseous and dissolved $CO_2$.

Sorption kinetics can be used to extract diffusion coefficients and to delineate the transport mechanism of $CO_2$ through the PMMA matrix. Figure 2 shows the reduced Raman intensity against square root of elapsed

---

[†] National Institute of Advanced Industrial Science and Technology.
[‡] National Research Council of Canada.
[§] Technology Center, Pactiv Corporation.
[⊥] Present address: Corporate R&D, LG Chem/Research Park, Daejeon 305-380, Korea.
[*] Corresponding authors: e-mail jihoyoon@lgchem.com or phanda@pactiv.com.

10.1021/ma048742q CCC: $27.50

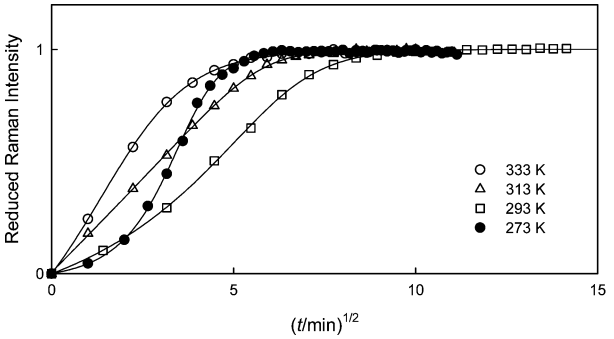

**Figure 2.** Sorption kinetics of $CO_2$ dissolved in PMMA as a function of $t^{1/2}$ at 3 MPa under various temperatures. The reduced Raman peaks of $CO_2$ molecules at 1385 $cm^{-1}$ were used for sorption kinetics.

time at four different temperatures and $CO_2$ pressure of 3 MPa. It is known from previous studies[1−6] that at 3 MPa PMMA−$CO_2$ is in the glassy state in the temperature range 278−333 K and in the rubbery state below 278 K, such that on heating at constant pressure from 273 K the system undergoes a rubber-to-glass transition and thence the retrograde behavior. Typical Fickian sorption kinetics characterized by the initial linear dependence on $t^{1/2}$ are observed at 313 and 333 K in Figure 2. This implies that the gas transport is controlled by a single parameter—the Fickian diffusion coefficient. Assuming Fickian transport,[17,18] the diffusion coefficients are estimated to be $2.5 \times 10^{-12}$ and $3.6 \times 10^{-12}$ $m^2\ s^{-1}$ at 313 and 333 K, respectively. These results agree well with the values in the range $1 \times 10^{-12}$−$3 \times 10^{-12}$ $m^2\ s^{-1}$ derived from sorption kinetics by gravimetric techniques.[8] In contrast, the sorption kinetics at 273 and 293 K reveal characteristic features that are commonly regarded as signatures for non-Fickian behavior. The sorption curves at 273 and 293 K exhibit sigmoidal shape similar to that reported in the past for a number of penetrant−glassy polymer systems.[19−24] This may be attributed to the formation of a plasticized front during the swelling process, resulting in the competing effects of Fickian diffusion and stress relaxation. Though the sigmoidal kinetics indicate non-Fickian behavior, it should be noted that the transport mechanism in the two cases is markedly different. At 293 K, the PMMA−$CO_2$ system is in the glassy state, and the polymer relaxation makes a minor contribution to controlling the overall gas transport. On the other hand, at 273 K, the outer shell of PMMA sphere in contact with $CO_2$ is transformed to the rubbery state whereas the inner core is still in the glassy state. Under these circumstances, the gas transport is controlled by the superimposition of contributions from the polymer relaxing on a time scale faster than the Fickian diffusion time scale and the velocity of the plasticized front on the underlying intrinsic Fickian diffusion.

It can be shown[17] that the distance $r$ between the surface of the spherical PMMA particle and the diffusion front is related to the evolution time $t$ via

$$r = kt^n \tag{1}$$

where $k$ is a constant related to the intrinsic diffusion coefficient and exponent $n$ is characteristic of the transport mode. For transport of small molecules through glassy polymers, $n = 0.5$ and refers to Fickian kinetics; $n$ is between 0.5 and 1.0 when the Fickian transport and polymer relaxation occur simultaneously, giving rise to the so-called anomalous behavior; and $n = 1.0$ for the case II transport whereby the penetrant swells the polymer, and this stress-induced relaxation front moves through the polymer at a constant velocity. Figure 3 shows images of the diffusion fronts in a spherical PMMA sample obtained using a microfocus X-ray CT scanner after conditioning the polymer with $CO_2$ for a given time followed by foaming at 95 °C. The formation of sharp fronts indicates that the inner core remains glassy, resulting in a significant difference in the diffusion coefficients between the inner (glassy) and outer (rubbery) regions. The dynamics of propagation of diffusion front can be often measured using optical methods for polymers interacting with a solvent or plasticizer.[25−28] However, the optical techniques can be applied only to transparent polymer−penetrant systems. On the other hand, the microfocus X-ray CT scanning technique to study the formation and dynamics of propagation of diffusion front applies to transparent as well as nontransparent matrices. More quantitative and precise data can be obtained from the X-ray CT scanning, in particular the kinetics of the diffusion and swelling processes, than by optical imaging.

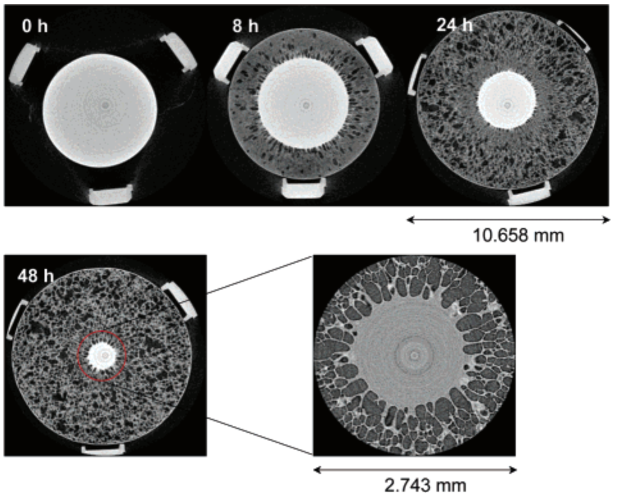

**Figure 3.** X-ray CT scanning of 6 mm PMMA samples. Each sample was exposed to compressed $CO_2$ at 273 K and 3 MPa for the given time interval and then instantly transferred to hot water to generate the foamed structure in the outer shells.

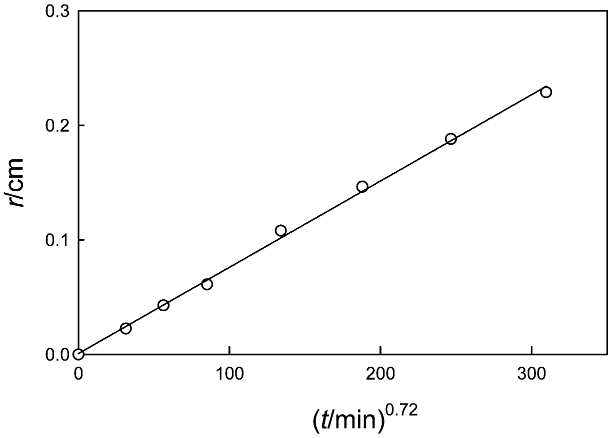

**Figure 4.** Diffusion front propagation in 6 mm PMMA samples obtained using X-ray CT at 273 K and 3 MPa.

The $r$−$t$ data obtained from the X-ray CT scans are shown plotted in Figure 4. The results indicate that the distance $r$ is not proportional to $t^{1/2}$ (Fickian diffusion) or $t$ (case II diffusion), but to $t^{0.72}$, thereby establishing the transport mechanism to be non-Fickian. This is consistent with the sorption kinetics observed by in-situ Raman spectroscopy as shown in Figure 2.

In conclusion, the experimental tools and the results presented here can be useful for developing a transport model that takes into account the competing effects of Fickian diffusion, stress relaxation, and phase transitions. The information on sorption kinetics obtained from the Raman spectra augmented with velocity of the plasticized front obtained from the X-ray CT scans can be used for developing processes to produce the desired cellular morphologies.

**Acknowledgment.** This work was completed while J.-H. Yoon was a JSPS fellow of the National Institute of Advanced Industrial Science and Technology and was funded by the JSPS fellowship program of the Japan Society for the Promotion of Science. We thank Drs. T. Uchida and Y. Sakamoto for their helpful comments on the Raman spectra.

## References and Notes

(1) Condo, P. D.; Sanchez, I. C.; Panayiotou, C. G.; Johnston, K. P. *Macromolecules* **1992**, *25*, 6119.
(2) Condo, P. D.; Johnston, K. P. *Macromolecules* **1992**, *25*, 6730.
(3) Wissinger, R. G.; Paulaitis, M. E. *J. Polym. Sci., Part B: Polym. Phys.* **1991**, *29*, 631.
(4) Kalospiros, N.; Paulaitis, M. E. *Chem. Eng. Sci.* **1994**, *49*, 659.
(5) Condo, P. D.; Johnston, K. P. *J. Polym. Sci., Part B: Polym. Phys.* **1994**, *32*, 523.
(6) Handa, Y. P.; Zhang, Z. *J. Polym. Sci., Part B: Polym. Phys.* **2000**, *38*, 716.
(7) Handa, Y. P.; Zhang, Z. US Patent No. 5,955,511.
(8) Handa, Y. P.; Zhang, Z.; Wong, B. *Cell. Polym.* **2001**, *20*, 1.
(9) Wong, B.; Zhang, Z.; Handa, Y. P. *J. Polym. Sci., Part B: Polym. Phys.* **1998**, *36*, 2025.
(10) Chang, S.-H.; Park, S.-C.; Shim, J.-J. *J. Supercrit. Fluids* **1998**, *13*, 113.
(11) von Schnitzler, J.; Eggers, R. *J. Supercrit. Fluids* **1999**, *16*, 81.
(12) Fleming, G. K.; Koros, W. J. *Macromolecules* **1986**, *19*, 2285.
(13) Nikitin, L. N.; Said-Galiyev, E. E.; Vinokur, R. A.; Gallyamov, M. O.; Schaumburg, K. *Macromolecules* **2002**, *35*, 934.
(14) Royer, J. R.; DeSimone, J. M.; Khan, S. A. *Macromolecules* **1999**, *32*, 8965.
(15) Zhang, Y.; Gangwani, K. K.; Lemert, R. M. *J. Supercrit. Fluids* **1997**, *11*, 115.
(16) Takahashi, M.; Yamamoto, Y.; Nawaby, A. V.; Handa, Y. P. *J. Polym. Sci., Part B: Polym. Phys.* **2003**, *41*, 2214.
(17) Crank, J. *The Mathematics of Diffusion*, 2nd ed.; Oxford University Press: Oxford, 1975.
(18) Carslaw, H. S.; Jaeger, J. C. *Conduction of Heat in Solids*, 2nd ed.; Oxford University Press: Oxford, 1946.
(19) Crank, J.; Park, G. S. *Trans. Faraday Soc.* **1949**, *45*, 240.
(20) Kokes, R. J.; Long, F. A.; Hoard, J. L. *J. Chem. Phys.* **1952**, *20*, 1711.
(21) Crank, J. *J. Polym. Sci.* **1953**, *11*, 151.
(22) Long, F. A.; Kokes, R. J. *J. Am. Chem. Soc.* **1953**, *75*, 2232.
(23) Long, F. A.; Thompson, L. J. *J. Polym. Sci.* **1955**, *15*, 413.
(24) Billovits, G. D.; Durning, C. J. *Polymer* **1988**, *29*, 1468.
(25) Colombo, P.; Bettini, R.; Peppas, N. A. *J. Controlled Release* **1999**, *61*, 83.
(26) Yamamoto, T.; Nozaki, K. *Polymer* **1995**, *36*, 2505.
(27) McHugh, A. J.; Miller, D. C. *J. Membr. Sci.* **1995**, *105*, 121.
(28) Morrissey, P.; Vesely, D. *Polymer* **2000**, *41*, 1865.

MA048742Q